ChemPubSoc Europe

DOI: 10.1002/chem.201601564

CHEMISTRY A European Journal Full Paper

Substituent Effects

Effect of Methyl, Hydroxyl, and Chloro Substituents in Position 3 of 3′,4′,7-Trihydroxyflavylium: Stability, Kinetics, and Thermodynamics

Alfonso Alejo-Armijo,[a] Sofía Salido,[a] Joaquín Altarejos,[a] A. Jorge Parola,*[b] Sandra Gago,[b] Nuno Basílio,[b] Luis Cabrita,[b] and Fernando Pina*[b]

Abstract: The effect of methyl, hydroxyl, and chloride substituents in position 3 of the 3′,4′,7-trihydroxyflavylium core structure was studied. The stability, relative energy of each of chemical species (thermodynamics), and their rates of interconversion (kinetics) are very dependent on these substituents. By comparing the mole fraction distribution at equilibrium of the three multistate systems with the parent 3′,4′,7-trihydroxyflavylium, introduction of a methyl substituent in position 3 increases the mole fraction of hemiketal at the expense of the *trans*-chalcone and increases the hydration rate very significantly; a hydroxyl substituent in position 3 gives rise to a degradation process, as observed in anthocyanidins. In the case of 3-chloro-3′,4′,7-trihydroxyflavylium, a dramatic increase of the flavylium cation acidity was observed and a photochromic system can be operated upon irradiation of the respective *trans*-chalcone in 1 M HCl. According to the photochromic response of 3,3′,4′,7-tetrahydroxyflavylium and 3′,4′,7-trihydroxyflavylium, some requirements for a good photochromic performance are discussed.

Introduction

Flavylium derivatives constitute a family of compounds that include anthocyanins, anthocyanidins, deoxyanthocyanidins, and numerous natural and synthetic compounds containing the flavylium core.[1–4] Some details of anthocyanin chemistry could be fully understood only after achievements obtained by the study of synthetic flavylium analogues.[5,6] On the other hand, flavylium derivatives can perform as photochromic systems,[1,7,8] both in solution and in more organized matrices,[9–13] as well as models for the development of optical memories.[1,14]

One interesting characteristic of flavylium derivatives is the existence of a common sequence of chemical reactions, as shown in Scheme 1 for malvidin-3-*O*-glucoside (oenin).[1,15–18]

The flavylium cation is only a stable species at very acidic pH values. Increasing the pH leads to the formation of several species (Scheme 1) through a series of chemical equilibria accounted for in Equations (1)–(4):

proton transfer :

$$AH^+ + H_2O \rightleftharpoons A + H_3O^+ \quad (K_a) \tag{1}$$

hydration :

$$AH^+ + 2\,H_2O \rightleftharpoons B + H_3O^+ \quad (K_h) \tag{2}$$

tautomerization :

$$B \rightleftharpoons Cc \quad (K_t) \tag{3}$$

isomerization :

$$Cc \rightleftharpoons Ct \quad (K_i) \tag{4}$$

The system can be simplified by considering a single acid–base equilibrium involving species AH^+ (acid) in equilibrium with a conjugate base (CB), with [CB] = [A] + [B] + [Cc] + [Ct] [Eqs. (5) and (6)].[1]

acid − base global equilibrium :

$$AH^+ + H_2O \rightleftharpoons CB + H_3O^+ \quad (K'_a) \tag{5}$$

$$K'_a = K_a + K_h + K_hK_t + K_hK_tK_i \tag{6}$$

In some cases (e.g., a high *cis–trans* isomerization kinetic barrier), it is possible to define a pseudo-equilibrium; a transient state in which all species except Ct (pseudo)equilibrate [Eqs. (7) and (8), with [CB^] = [A] + [B] + [Cc]].

acid − base pseudo-equilibrium :

$$AH^+ + H_2O \rightleftharpoons CB\hat{} + H_3O^+ \quad (K\hat{}_a) \tag{7}$$

[a] A. Alejo-Armijo, Dr. S. Salido, Prof. J. Altarejos
Departamento de Química Inorgánica y Orgánica
Facultad de Ciencias Experimentales, Universidad de Jaén
23071 Jaén (Spain)

[b] Dr. A. J. Parola, Dr. S. Gago, Dr. N. Basílio, Dr. L. Cabrita, Prof. F. Pina
LAQV, REQUIMTE, Departamento de Química
Faculdade de Ciências e Tecnologia, Universidade NOVA de Lisboa
2829-516 Caparica (Portugal)
E-mail: ajp@fct.unl.pt
fp@fct.unl.pt

Supporting information and ORCIDs from the authors for this article are available on the WWW under http://dx.doi.org/10.1002/chem.201601564.

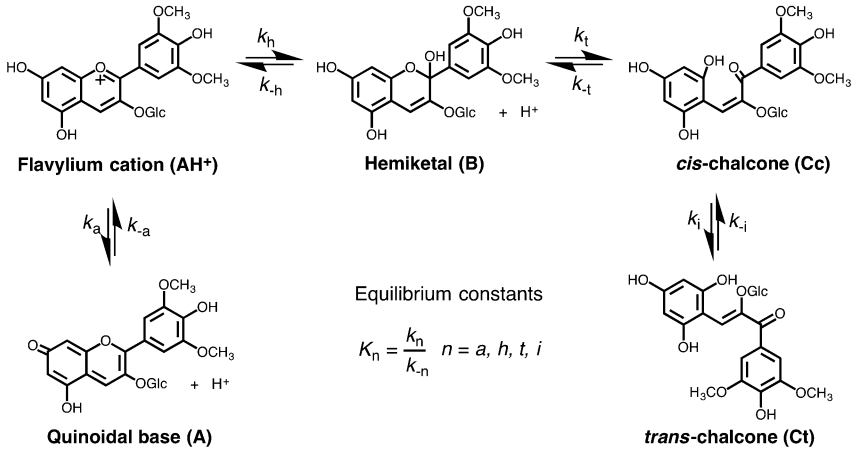

Scheme 1. The chemical reaction network established by malvidin-3-*O*-glucoside (oenin) in aqueous solution illustrates the multistate system characteristics of flavylium cations.

$$\hat{K_a} = K_a + K_h + K_h K_t \quad (8)$$

A few years ago, we introduced energy-level diagrams as a very convenient way to visualize these multistate systems (Scheme 2). It is easily constructed provided that all equilibrium constants in Scheme 1 [Eqs. (1)–(4)] were previously determined. A detailed explanation of its construction is reported in reference [19].

Following the energy-level diagram in Scheme 2, it is easy to confirm that at low pH values the flavylium cation (AH+) is the stable species. By raising the pH, for example, to pH = pK_a, 50% of each AH^+ and A are formed because proton transfer is by far the fastest reaction of the multistate system. The AH^+ and A species are in fast equilibrium and thus behave as a single species in subsequent kinetic steps. Brouillard and Dubois, who discovered that in acidic medium the quinoidal base, A, did not hydrate, made an important breakthrough in the comprehension of flavylium multistate kinetics.[18] In other words, the evolution towards equilibrium is exclusively made by means of the hydration of AH^+ to give the hemiketal (B). The hemiketal then tautomerizes to form the *cis*-chalcone (Cc), which finally isomerizes to yield the *trans*-chalcone (Ct).

The most practical way to study the flavylium-based chemical reaction network is to carry out direct pH jumps, which are defined as the addition of base to equilibrated solutions of AH^+ at sufficiently low pH values at which it is the sole species. In addition, reverse pH jumps, which are defined as the addition of acid to solutions equilibrated at higher pH values to give back AH^+, are also very useful. In both cases, the process is usually followed by UV/Vis spectrophotometry; when the reactions take place on a timescale of seconds up to milliseconds, a stopped flow is required.

After a direct pH jump, base A is formed upon proton transfer to the solvent, in a process with a rate constant of the order of microseconds; a rate not measurable by stopped flow. The next step is the disappearance of AH^+/A through the hydration of AH^+ followed by tautomerization, occurring on the subsecond timescale. When there is a *cis*–*trans* isomerization

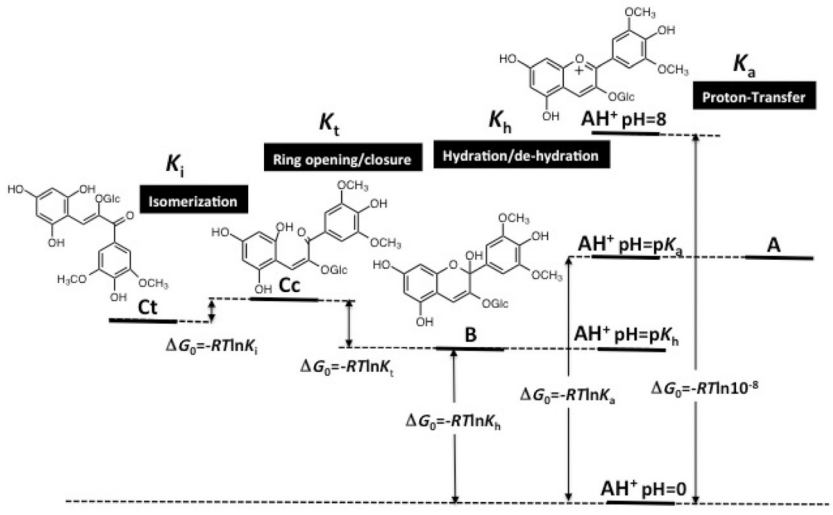

Scheme 2. Energy-level diagram of the oenin multistate system in aqueous solution.[19]

barrier, after this process all species of the multistate are in equilibrium, except Ct. In other words, once B is formed it immediately gives Cc and at this point species AH^+, A, B, and Cc are in a metastable state that is called a pseudo-equilibrium [Eqs. (7) and (8)]. Finally, from the pseudo-equilibrium, the equilibrium is achieved upon the *cis–trans* isomerization of Cc to yield Ct. This process may occur on a timescale from subseconds to days and will control the global rate of the equilibration process. The kinetic expressions to account for the three kinetic steps are given by Equations (9)–(11):[1,19]

$$k_1 = k_a + k_{-a}[H^+] \tag{9}$$

$$k_2 = \frac{[H^+]}{[H^+] + K_a} k_h + \frac{1}{1 + K_t} k_{-h}[H^+] \tag{10}$$

$$k_3 = \frac{K_h K_t}{[H^+] + K_a + K_h + K_h K_t} k_i + k_{-i} \tag{11}$$

Tautomerization is generally faster than hydration, except for very acidic pH values, as observed in reverse pH jumps or even in direct pH jumps. In the former case, two kinetic processes are observed given by Equations (12) and (13):[20]

$$k_4 = \frac{[H^+]}{[H^+] + K_a} k_h + k_{-h}[H^+] \tag{12}$$

$$k_5 = k_{-t} \tag{13}$$

In the latter case (less common), the equilibrium AH^+/A/B is established before ring opening/closure and Equation (14) holds:

$$k_6 = \frac{K_h}{[H^+] + K_a + K_h} k_t + k_{-t} + k_t^H[H^+] \tag{14}$$

in which k_t^H accounts for the acidic catalysis of ring opening/closure.[5,6]

When the *cis–trans* isomerization barrier is small, the system is equivalent to three species in equilibrium, X⇄Y⇄Z, and Equations (15) and (16) can be deduced:[21]

$$A \underset{H^+}{\overset{K_a}{\rightleftharpoons}} AH^+ \underset{k_{-h}[H^+]}{\overset{k_h}{\rightleftharpoons}} B \overset{K_t}{\rightleftharpoons} Cc \underset{k_{-i}}{\overset{k_i}{\rightleftharpoons}} Ct \tag{15}$$

$$k_{obs} = \frac{\frac{[H^+]}{[H^+]+K_a} K_h K_t k_i + k_{-i}[H^+]}{\frac{k_i K_t}{k_{-h}} + [H^+]} \tag{16}$$

Herein, three new flavylium derivatives, 3,3′,4′,7-tetrahydroxyflavylium (**F1**), 3′,4′,7-trihydroxy-3-methylflavylium (**F2**), and 3-chloro-3′,4′,7-trihydroxyflavylium (**F3**), were synthesized and their stability, thermodynamics, and kinetics studied and compared with similar flavylium derivatives reported in the literature (Scheme 3).

The synthesis of 3-substituted flavylium salts is of great interest because their reaction with π-nucleophilic units (i.e., catechin) could open up a route to prepare A-type proanthocyanidins or analogues.[22] To achieve the synthesis of such unusual bridged structures present in the A-type oligocatechins from appropriate flavylium salts, a study of the properties of the starting flavylium cations is required.

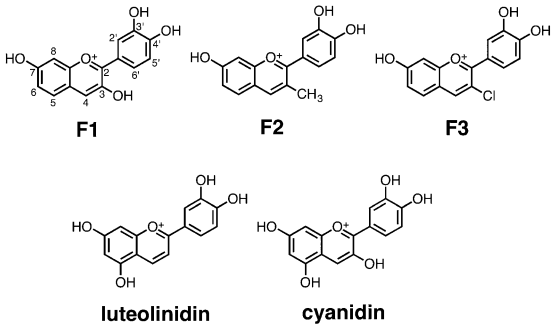

Scheme 3. From left to right: 3,3′,4′,7-tetrahydroxyflavylium (**F1**), 3′,4′,7-trihydroxy-3-methylflavylium (**F2**), 3-chloro-3′,4′,7-trihydroxyflavylium (**F3**), 3′,4′,5,7-tetrahydroxyflavylium (luteolinidin), and 3,3′,4′,5,7-pentahydroxyflavylium (cyanidin).

Results and Discussion

3,3′,4′,7-Tetrahydroxyflavylium (F1)

The stability of **F1** in moderately acidic solutions was checked according to the following sequence of events: 1) a direct pH jump from a solution of the compound equilibrated at pH 1.15 to pH 4.40; 2) this solution was kept for 20 min (the experiment was repeated for longer times); and 3) a reverse pH jump to pH 1.17 (Figure 1a). The respective kinetics of flavylium cation recovery was then monitored (Figure 1b). The kinetic process reported in Figure 1b recovers only about 2% of the initial flavylium. At the end of the kinetics reported in Figure 1b, 10% of the flavylium cation was not recovered, which indicated that a decomposition process took place at pH 4.40. This behavior, to a lesser extent, shows similarities with the degradation of cyanidin (Scheme 3) recently reported (Figure 1c).[23] A direct pH jump from pH 0.8 to 4.6, waiting 20 min at this pH, followed by a reverse pH jump back to pH 0.9, gave rise to more than 95% degradation. In other words, less than 5% of flavylium cations were recovered after this process.

The absorption spectrum 3 h after a direct pH jump from pH 1 to pH 3.2 is shown in Figure 2a. The corresponding spectrum after one month is given in Figure 2b. Acidification of this last solution leads to spectrum Figure 2c, which is coincident with that of Figure 2b. Clearly, no flavylium is recovered and the final product after one month at pH 3.2 is not dependent on pH (in this range). Conversely, luteolinidin possessing a hydroxyl substituent in position 5 (but not in position 3; Scheme 3) is relatively stable.[24] This result corroborates that the degradation process in anthocyanidins is due to the existence of the hydroxyl substituent in position 3, with a suggested mechanism involving the formation of a 3,4-diketone that breaks down in two carboxylic acids.[23] By analogy, compound **F1** would expectedly degrade into 2,4- and 3,4-dihydroxybenzoic acid.

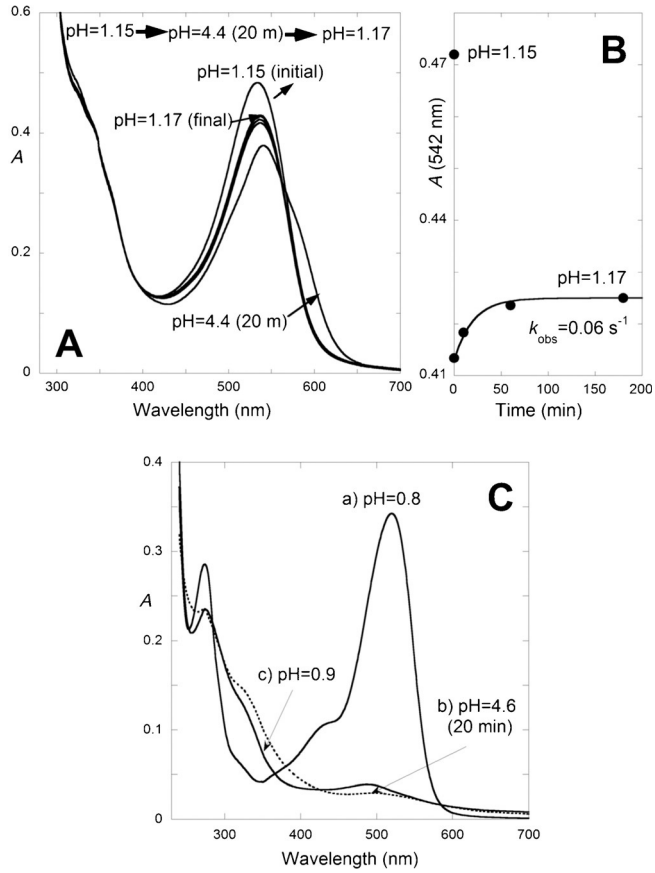

Figure 1. a) Spectral variations of a 1.3×10^{-4} M solution of **F1** in water/methanol (1:1) upon a direct pH jump from pH 1.15 to pH 4.40 (standing 20 min) followed by a reverse pH jump back to pH 1.17. b) Kinetics of flavylium recovery. At the end of this process, only 90% of flavylium cations were recovered. c) Cyanidin spectral variations upon a direct pH jump from pH 0.8 to pH 4.6 (standing 20 min) followed by a reverse pH jump back to pH 0.9.

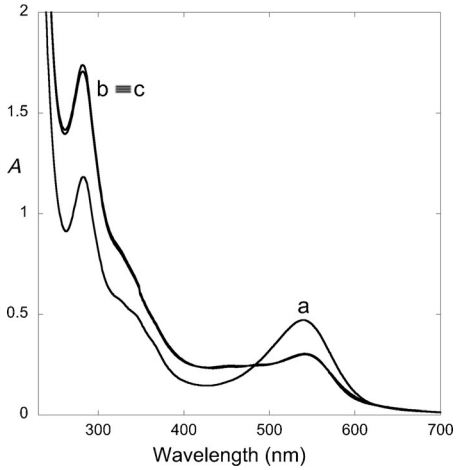

Figure 2. Absorption spectra of a 1.3×10^{-4} M solution of **F1** in water/methanol (1:1) after a direct pH jump to 3.2: a) after 3 h; b) after 1 month; c) the same as that of b) at pH 1.

The number and position of hydroxyl substituents in the flavylium core accounts for the different colors of the compounds. Table 1 shows that introduction of hydroxyl substituents in any position of the flavylium core redshifts the maximum of the flavylium cation; a phenomenon already described for anthocyanins.[28] The red color is obtained only for **F1**. The solubility of this compound is low in water or mixtures of water and organic solvents, which prevents the use of NMR spectroscopy and the study of other deprotonation equilibria taking place at neutral and basic pH values.

Table 1. Absorption maximum of hydroxyl-substituted flavylium cations.

Cation	λ [nm]
_[8][a]	394
7-OH[25]	435
4′-OH[25]	435
4′,7-di-OH[26]	458
3′,4′,7-tri-OH[27]	469
3,3′,4′,7-tetra-OH[b]	531

[a] Flavylium with no substituents. [b] This work.

3′,4′,7-Trihydroxy-3-methylflavylium (F2)

The sequence of spectral variations accompanying direct pH jumps for **F2** ($\lambda_{max}=478$ nm) are reported in Figure 3.

The quinoidal base ($\lambda_{max}=525$ nm) is formed during the mixing time of the base added to equilibrated solutions of flavylium cation, at pH 1.0, as shown in Figure 3a; the spectra were monitored by stopped flow 10 ms after mixing. The inflection point of the trace in the inset corresponds to the pK_a of the flavylium cation–quinoidal base acid–base equilibrium, p$K_a=4.3$. It is expected that the quinoidal base forms on position 7 (as shown in Scheme 1 for oenin), which is known to be more acidic than the 4′-position.[1]

The pH-dependent spectral variations at pseudo-equilibrium are shown in Figure 3b and again the system behaves as a single acid–base equilibrium involving AH^+ and CB^ [Eq. (7)]. Finally, equilibrium is reached in a few hours, corresponding to a single acid–base equilibrium involving AH^+ and CB [eq. (5)].

Taking into account [see Eqs. (6) and (8)] that $K'_a-K^{\wedge}_a=K_hK_tK_i=1.5\times10^{-3}$ M, the fraction of Ct in CB can be calculated as $K_hK_tK_i/K'_a=0.6$. Moreover, the ratio K_a/K'_a predicts a fraction of 0.05 of the base at equilibrium, which is in good agreement with spectral variations and the data of the direct pH jumps (Figure 3c). Thus, a fraction of 0.35 should be assigned to the mole fractions of B and Cc.

From the initial state of the system represented in Figure 3a containing only AH^+ and A, the multistate system evolves towards equilibrium through a complex kinetic process. The pH jumps monitored over time allow three kinetic steps to be distinguished (Figure 4).

The faster processes were followed by stopped flow (Figure 4a), data for which could be fitted with biexponential laws. For instance, a pH jump from 1.0 to 3.6 is fitted with $k_{obs1}=0.42\ s^{-1}$, which is compatible with the hydration process [at this pH value, hydration is faster than tautomerization, due to its direct dependence on proton concentration; Eq. (10)] and $k_{obs2}=0.029\ s^{-1}$; this can be assigned to the tautomerization

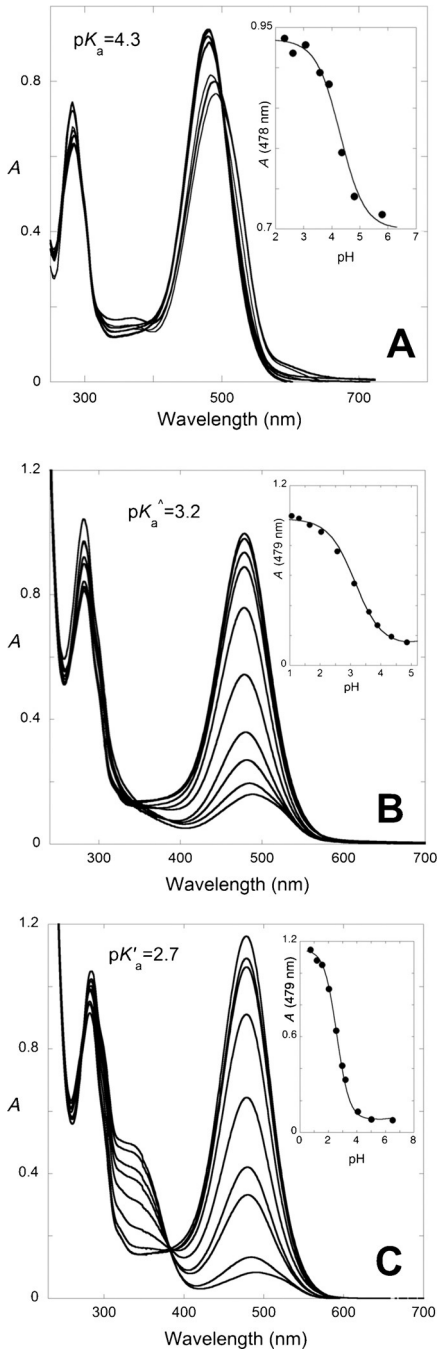

Figure 3. The pH-dependent spectral variations of **F2** in ethanol/water (1:1) upon pH jumps from a stock solution at pH 1.2 to higher pH values: a) 10 ms after a direct pH jump, followed by stopped flow ($pK_a = 4.3$, 5.6×10^{-5} M); b) at pseudo-equilibrium ($pK^{\wedge}_a = 3.2$, 5.3×10^{-5} M); c) at equilibrium ($pK'_a = 2.7$, 6.5×10^{-5} M).

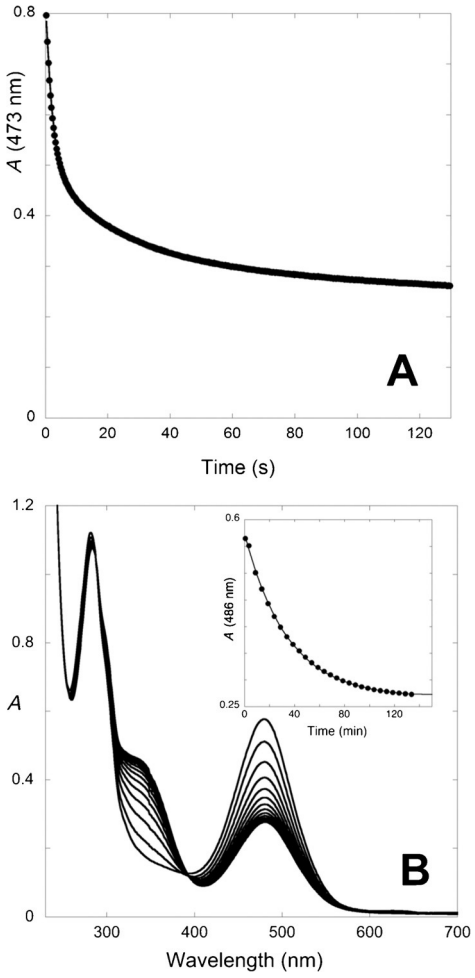

Figure 4. a) Trace of the absorbance at $\lambda = 473$ nm of **F2** in water/ethanol (1:1) upon a direct pH jump from 1.0 to 3.6, 5.6×10^{-5} M, followed by stopped flow; the trace can be fitted with a biexponential law with rate constants of 0.42 s^{-1} and 0.029 s^{-1}, which can be assigned to hydration and tautomerization, respectively. b) The same measurements as those in a) for pH 1.0 to 3.7, 6.5×10^{-5} M, obtained on a common spectrophotometer; fitting was achieved with a monoexponential law with a rate constant of 4.8×10^{-4} s^{-1}, which was assigned to isomerization.

equilibrium. On a slower timescale, followed by using a spectrophotometer, a third step was observed and attributed to *cis–trans* isomerization, with $k_{obs3} = 4.8\times10^{-4}$ s^{-1}.

A series of direct pH jumps to several pH values permits the hydration (k_{obs1}) and tautomerization (k_{obs2}) processes to be fitted with Equations (10) and (14), respectively (Figure 5 a). The last step to reach equilibrium is controlled by isomerization and can be accounted for by Equation (11). Fitting was achieved with the rate and equilibrium constants reported in Table 2 with excellent agreement.

Direct pH jumps are conveniently complemented by reverse pH jumps (Figure 6). The trace for flavylium formation shows two kinetic processes. The species constituting CB at pH 6 are in equilibrium and after the pH jumps back to 1.7, for example, A is immediately transformed into AH^+. This step occurs during the mixing time of the stopped flow. The first kinetic step observed in Figure 6 a corresponds to the formation of AH^+ from B. The observed rate constant is in very good agreement with the value expected from Equation (12). The last step can be assigned to ring closure [k_{-t}; Eq. (13)] because there is no equilibrium between B and Cc. In other words, once B is formed, it disappears to give AH^+. The amplitude of the exponentials permits $K_t = 0.68$ to be calculated. On the other hand, the tautomerization reaction is catalyzed by acids and bases.[5,6] Although the equilibrium constant is the same, the

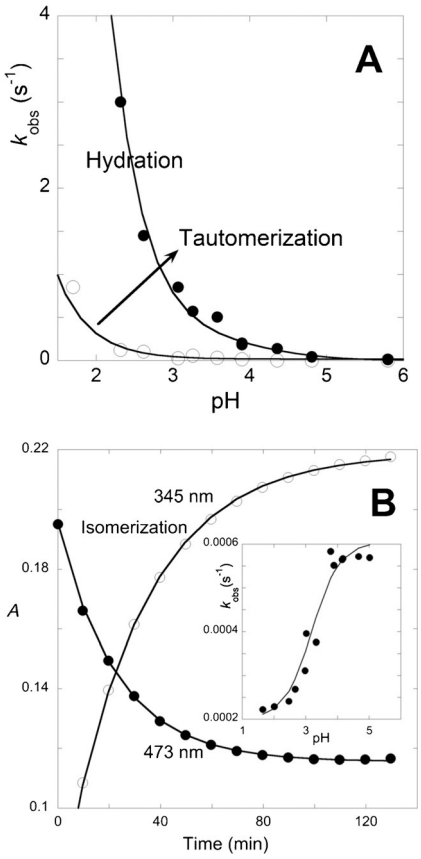

Figure 5. a) The pH dependence of hydration [●; Eq. (10)] and tautomerization [○; Eq. (14)]; fitting was achieved for $k_h = 0.3\ s^{-1}$, $k_{-h} = 600\ M^{-1}s^{-1}$, $pK_a = 4.3$, $k^H_t = 40\ M^{-1}s^{-1}$; there is not enough accuracy to determine k_t and k_{-t}. b) Trace of the AH^+ ($\lambda = 473$ nm) and CB ($\lambda = 345$ nm) absorption changes that correspond to the slowest kinetic step of a direct pH jump to 3.9; fitting of the inset was achieved with Equation (11) for $K^{\wedge}_a = 10^{-3.2}$, $K_t = 0.7$, $K_h = 5.0\times10^{-4}\ M^{-1}s^{-1}$, $k_i = 7.0\times10^{-4}\ s^{-1}$, $k_{-i} = 2.0\times10^{-4}\ s^{-1}$; these results are in good agreement with data from other experiments, see Table 2.

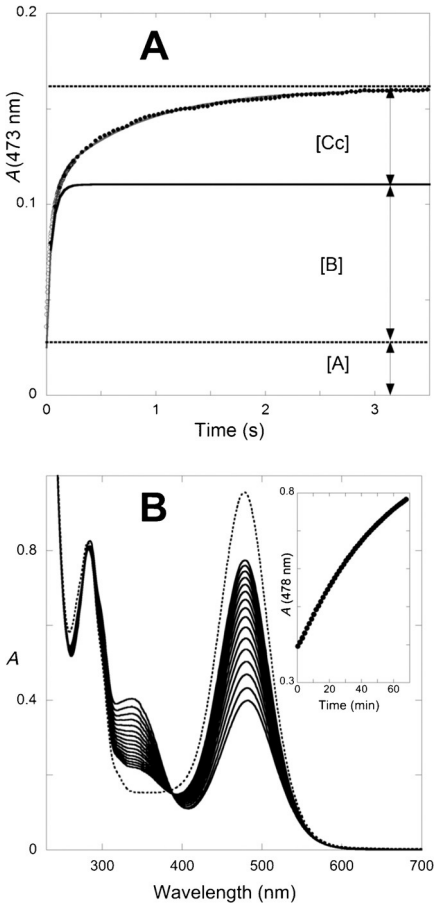

Figure 6. a) Reverse pH jump from pH 6.0 to 1.7; trace for flavylium cation formation followed by stopped flow at $\lambda = 473$ nm (2.8×10^{-5} M). The ratio between the amplitudes of Cc and B permits the equilibrium constant to be calculated: $K_t = 0.68$. Fitting was achieved for $k_1 = 20\ s^{-1}$ and $k_2 = 1.26\ s^{-1}$. b) Reverse pH jump from pH 5.4 to 1.2 (5.3×10^{-5} M); line corresponds to the final spectrum at pH 1.2. The system evolves to AH^+ according to a monoexponential law with a rate constant equal to $2.7\times10^{-4}\ s^{-1}$. The ratio of the exponential amplitudes and final absorbance leads to a mole fraction of Ct = 0.6 at pH 5, which is in agreement with the fraction obtained from the data shown in Figure 3c.

Table 2. Equilibrium constants in water/methanol (1:1).[a]

	pK'_a	$pK^{\wedge}_a$	pK_a	K_h [M]	K_t	K_i
3,3′,4′,7-tetra-OH (**F1**)	2.5	2.88	2.9	–	–	–
3′,4′,7-tri-OH[27]	3.1	4.3	4.1	7.6×10^{-7}	0.29	3.5×10^{3}
3-Me-3′,4′,7-tri-OH (**F2**)	2.7	3.2	4.3	5.0×10^{-4}	0.7	3.5

[a] Estimated error 20%.

Table 3. Rate constants in water/methanol (1:1).[a]

	k_h [s^{-1}]	k_{-h} [$M^{-1}s^{-1}$]	k_t [s^{-1}]	k_{-t} [s^{-1}]	k_i [s^{-1}]	k_{-i} [s^{-1}]
3,3′,4′,7-tetra-OH (**F1**)	0.0027	100	–	–	–	–
3′,4′,7-tri-OH[27]	0.013	1.7×10^{4}	0.23	0.8	0.7	2.0×10^{-4}
3-Me-3′,4′,7-tri-OH (**F2**)[c]	0.3	600	0.007[b]	0.01[b]	7×10^{-4}	2×10^{-4}

[a] Estimated error 20%. [b] At pH 1.7 under acidic catalysis. [c] Water/ethanol (1:1).

rate constants increase with increasing pH, and thus, the values reported in Table 3 refer to pH 1.7. From Equation (14), it is possible to calculate $k^H_t = 40\ M^{-1}s^{-1}$; the constant accounts for acidic catalysis.

A global fitting of the data allows all of the rate and equilibrium constants of the multiequilibria to be calculated (Tables 2 and 3).

The mole fraction distribution for **F2** is shown in Scheme 4, in comparison with three other compounds: unsubstituted flavylium (**1**), 3-methylflavylium (**2**), and 4′,7-dihydroxy-3-methylflavylium (**3**). The introduction of a methyl group in position 3 of the flavylium core leads to a dramatic change to the mole fraction distribution of the CB species, leading to stabilization of hemiketal B, see compounds **1** and **2**. Differently, the addition of hydroxyl substituents to the flavylium structure decreases species B at the expense of Ct, see compounds **3** and **F2**.

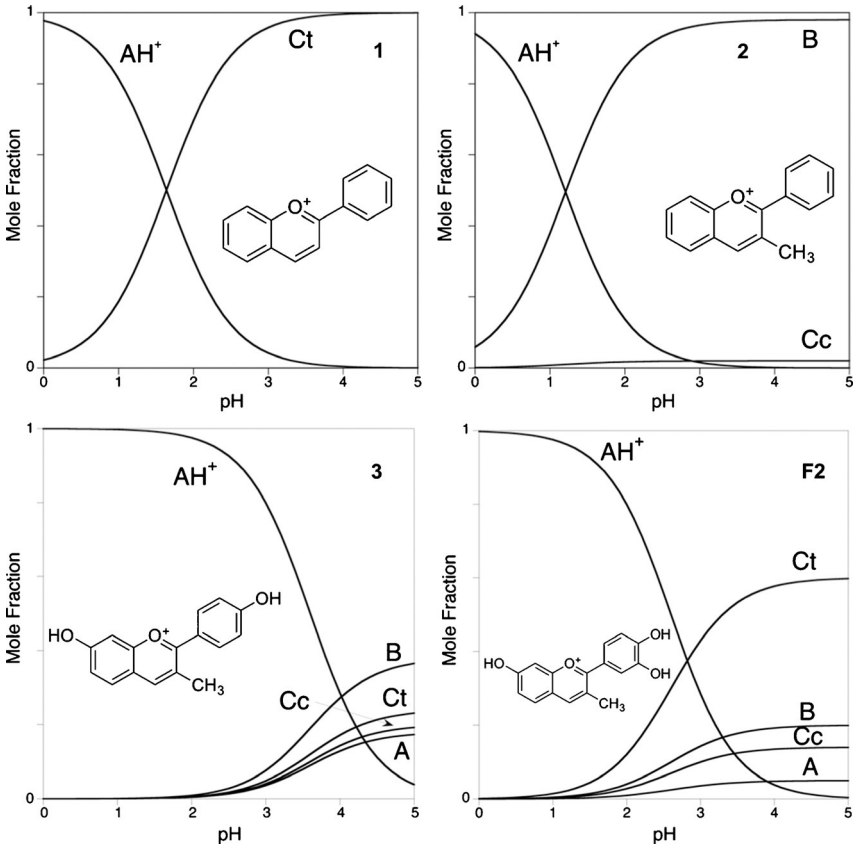

Scheme 4. Mole fraction distribution of flavylium compound[1] (**1**; water); 3-methylflavylium[29] (**2**; water); 4′,7-dihydroxy-3-methylflavylium[29] (**3**; water); and **F2** (this work, ethanol/water (1:1)).

3-Chloro-3′,4′,7-trihydroxyflavylium (F3)

Equilibrated solutions of **F3** at acidic pH values (Figure 7) reveal a dramatic shift of the global acidity of AH^+ towards extremely low pK'_a values ($pK'_a \approx -0.65$). The increase of AH^+ acidity can be explained by the high electronegativity of the chlorine substituent in position 3 ($-I$ inductive effect), rendering the system more reactive to hydration and deprotonation. In the case of **F1**, in which hydroxyl is present in position 3, although oxygen is similar in electronegativity to chlorine ($-I$), the hydroxyl group is also an electron π donor ($+M$ mesomeric effect). The overall effect reflects in the pK'_a values being similar to those of 3′,4′,7-trihydroxyflavylium and **F2** (Table 2), in which the 3-substituent is hydrogen and a methyl group, respectively (slight $+I$ inductive effect).

In the case of **F3**, it is very difficult to carry out rigorous experiments because the flavylium cation should be stored at [HCl] > 10 M. This extreme acidity makes it very difficult to control direct pH jumps. Moreover, at higher pH values decomposition is observed. We have measured the absorption spectra under very acidic conditions and the system is compatible with the equilibrium between flavylium cation, quinoidal base, and Ct. Photochemical experiments were carried out in ethanol/water (1:1) at pH 3.9 and in ethanol/1 M HCl (1:1; Figure 8). In the first case, the proton concentration is not sufficient to reach the thermodynamic level of the flavylium cation, and thus, only the disappearance of Ct (at $\lambda \approx 380$ nm) is detected

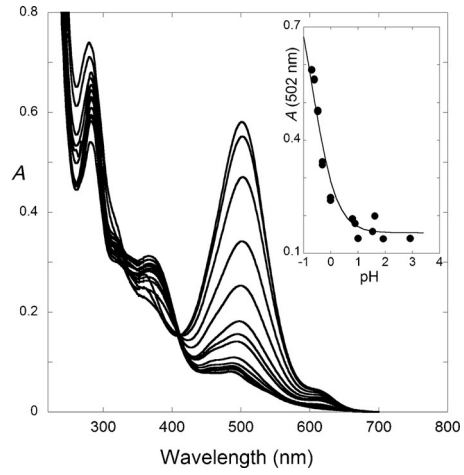

Figure 7. Spectral variations of equilibrated solutions of 5.6×10^{-5} M **F3** in ethanol/water (1:1); $pK'_a \approx -0.65$.

(Figure 8a). In the second case, the appearance of the flavylium cation is observed (Figure 8b). Two interesting aspects of this photochromic system should be highlighted: 1) it works at extremely high proton concentrations; and 2) due to the high proton concentration, the thermal back reaction is very fast and as a consequence the photochromic system is reversible (Figure 8b, inset). In spite of the harsh acidic conditions, the

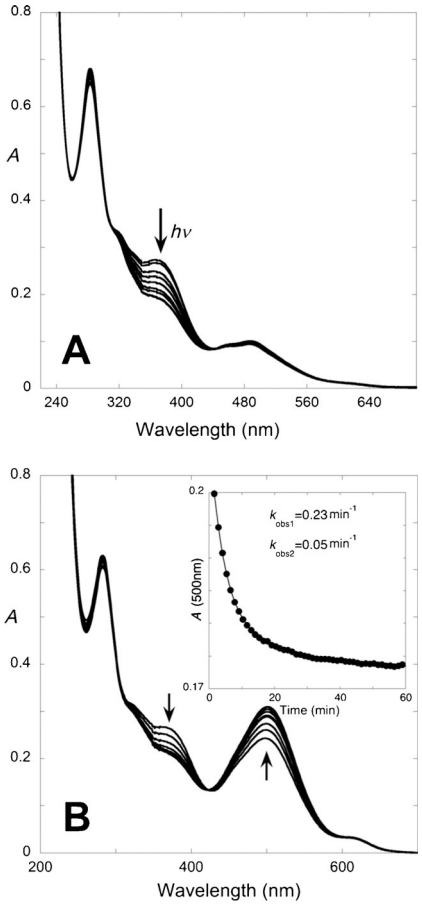

Figure 8. Irradiation of **F3** at $\lambda = 370$ nm in: a) ethanol/water (1:1), pH 3.9, 5.6×10^{-5} M, 22 min total irradiation time; b) ethanol/1 M HCl (1:1), 5.6×10^{-5} M, 10 min total irradiation time; inset: thermal recovery. $I_0(\lambda = 370\ \text{nm}) = 2.8\times10^{-7}$ Einstein min^{-1}.

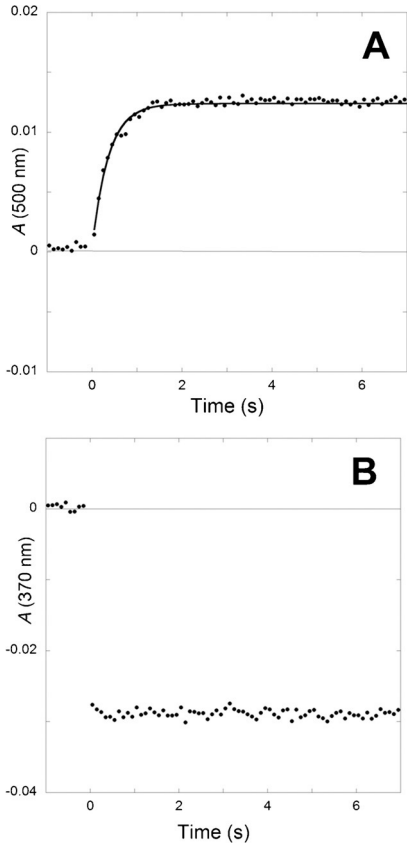

Figure 9. Flash photolysis of 5.6×10^{-5} M **F3** in ethanol/1 M HCl (1:1) at: a) $\lambda = 500$ nm (AH^+ absorption), $k = 2.8\ s^{-1}$; and b) $\lambda = 370$ nm (Ct absorption).

system loses less than 5% efficiency after 6 irradiation cycles (see the Supporting Information).

The results of flash photolysis experiments are reported in Figure 9. The trace corresponding to the formation of AH^+ fits to a monoexponential process with a rate constant of 2.8 s^{-1}, which indicates that the tautomerization of Cc gives B and the subsequent reaction of B gives AH^+. It is notable that the lack of recovery of the Ct absorption after the flash shows that isomerization (backward reaction) is much slower than the two forward processes to give the flavylium cation. However, isomerization (thermal back reaction) is faster than the other flavylium systems reported to date.[1] The color contrast of the photochromic system is relatively small, but it serves to illustrate the possibility of having a photochromic system operating at such high concentrations of proton.

On the design of photochromic systems

To rationalize the photochromic behavior of **F2** and compare it with the analogue lacking the methyl group in position 3, it is very convenient to draw an energy-level diagram (Scheme 5).

Irradiation of Ct leads to Cc, which spontaneously equilibrates with B and AH^+/A. The efficiency of the photochromic system measured by the maximum amount of color (AH^+ and A) reached by the system is illustrated in Figure 10. In the case of **F2** (Figure 10a), Cc and B have similar energies to the flavylium cation at pH 4.1, and thus, the appearance of the colored AH^+ and A species is limited. A better performance can be achieved at lower pH values, but in that case the initial fraction of flavylium cations increases, and thus, the color contrast is compromised. In the second case, in which the 3-methyl group is lacking, the situation is much more favorable from the point of view of the color appearance (Figure 10b). At pH 4.6, the flavylium cation is much lower in energy than B and Cc, and thus, more color can grow upon irradiation. However, the quantum yield for flavylium formation in the case of 3′,4′,7-trihydroxyflavylium ($\Phi = 0.02$ at pH 4.6) is lower than the value of $\Phi = 0.05$ observed for **F2** at pH 4.1. Moreover, at this pH, species B, Cc, and Ct are at roughly the same energy level, and thus, the amount of flavylium formed is only one-third of the total disappearance of Ct and the real quantum yield should be around 0.15. This is explained by comparing the rates of the primary photoproduct disappearance in both cases. In **F2**, the ratio between the forward and backward reactions is >85 and there is practically no back reaction at this stage of the process, whereas in 3′,4′,7-trihydroxyflavylium that ratio is only 1.4 and a significant fraction of Cc gives back Ct immediately after the flash.

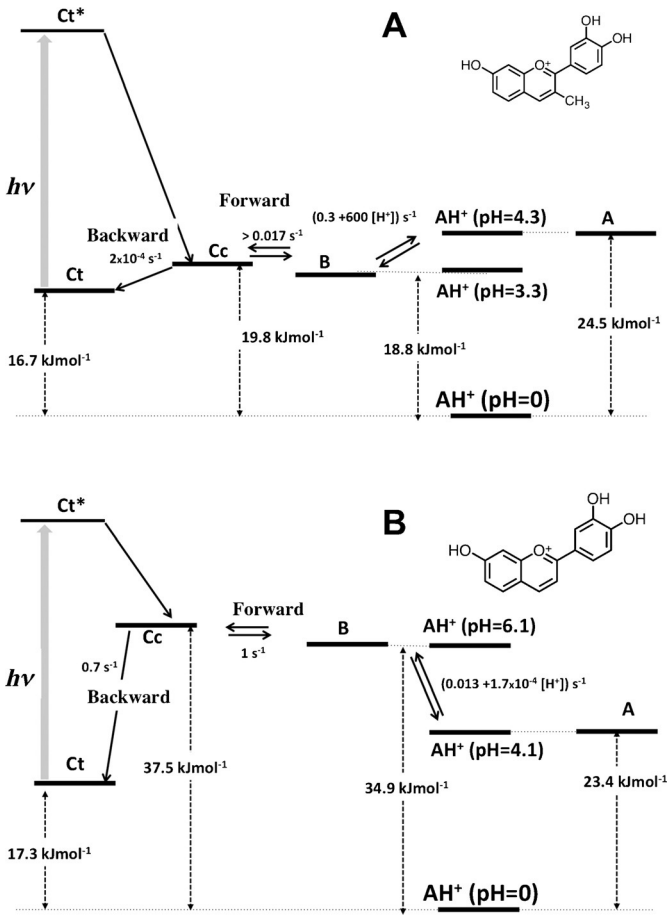

Scheme 5. Energy-level diagram for **F2** (top) and 3′,4′,7-trihydroxyflavylium (bottom); the light excitation arrows are not to scale.

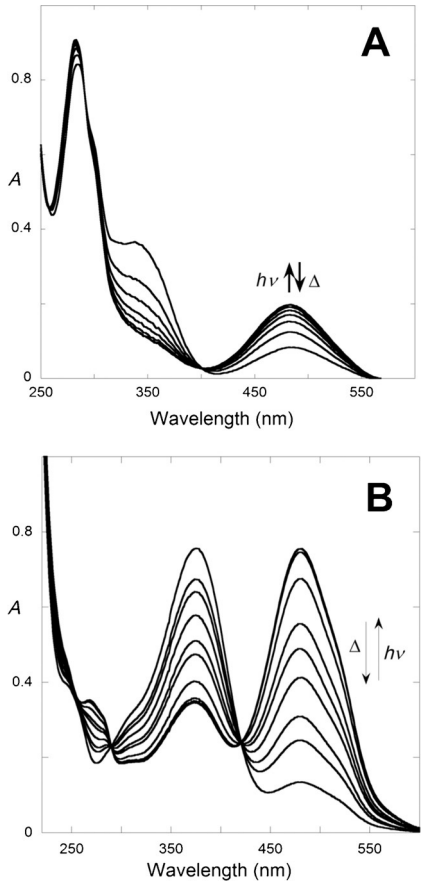

Figure 10. a) Spectral variations of **F2** (5.6×10^{-5} M) upon irradiation at $\lambda = 340$ nm, ethanol/water (1:1), pH 4.1, $\Phi = 0.05$, 13 min total irradiation time; $I_0(\lambda = 340\ \text{nm}) = 2.0\times10^{-7}$ Einstein min^{-1}. b) Spectral variations of 3′,4′,7-trihydroxyflavylium (3.5×10^{-5} M), pH 4.6, $\Phi = 0.02$, 11 min total irradiation time; $I_0(\lambda = 366\ \text{nm}) = 1.9\times10^{-6}$ Einstein min^{-1}.

The best performance for a photochromic system based on the flavylium reaction network is reached when B and Cc possess higher energy levels relative to that of Ct, along with a favorable ratio between the forward/backward reactions to prevent the recovery of Ct from Cc.

Conclusions

The study of the thermodynamics and kinetics of flavylium derivatives by constructing energy-level diagrams is an essential tool to rationalize the overall behavior of these compounds in solution. The stability, pH-dependent mole fraction distribution of species, and possible applications as photochromic systems, molecular-level optical memories, and reagents for the synthesis of higher-level flavonoids are strongly dependent on the nature and position of the substituents. The introduction of three different substituents, hydroxyl, methyl, and chlorine, in the 3-position of 3′,4′,7-trihydroxyflavylium leads to dramatically different behavior of the thermal and photochemical reactivity in alcoholic aqueous solutions showing that for synthetic flavylium compounds there is still a great field of progression and systematization to optimize the synthesis according to achievements required for practical applications of these compounds.

Experimental Section

General

All solvents and chemicals employed for synthesis and the preparation of samples were of reagent or spectrophotometric grade and were used as received; Millipore-grade water was used. NMR spectra were run on a Bruker AMX 400 instrument operating at 400.13 (^{1}H) and 100.00 MHz (^{13}C). Elemental analyses were performed on a Thermofinnigan Flash EA 112 series instrument.

Synthesis of 2,3′,4′-triacetoxyacetophenone

This compound was prepared according to a procedure reported in the literature for a similar compound, 2,4′-diacetoxyacetophenone.[30] Potassium acetate (14.3 mmol, 1.4 g) was added to a stirred solution of 2-chloro-3′,4′-dihydroxyacetophenone (10.7 mmol, 2.0 g) in acetic anhydride (20 mL). The reaction mixture was heated at 100 °C overnight. Then, crushed ice was added and a white solid precipitated. The solid was filtered off and carefully washed with water and dried, yielding 2,3′,4′-triacetoxyacetophenone (2.187 g, 7.4 mmol, 69%). ^{1}H NMR ($CDCl_3$): $\delta = 7.84$ (br d, ^3J(H5′,H6′) = 8.3 Hz, 1H; $H_{6'}$), 7.79 (br s, 1H; $H_{2'}$), 7.36 (d, ^3J(H5′,H6′) = 8.3 Hz, 1H; $H_{5'}$), 5.30 (s, 2H; -CO-CH_2-OAc), 2.34 (s, 6H; OAc), 2.24 ppm (s, 3H; OAc).

Synthesis of F1

This compound was prepared by condensation of 2,4-dihydroxybenzaldehyde (4.0 mmol, 0.552 g) and 2,3′,4′-triacetoxyacetophenone (4.0 mmol, 1.179 g). The reagents were dissolved in acetic acid (5 mL), and 98% H_2SO_4 (1.2 mL) was added. The reaction mixture was stirred overnight. Then, diethyl ether was added and a red solid precipitated. The solid was filtered off and carefully washed with diethyl ether and dried. The solid was recrystallized by dissolving it in EtOH/H_2O containing a few drops of $HClO_4$ (70%), yielding **F1** (0.592 g, 1.60 mmol, 40%). ^{1}H NMR (DCl/CD_3CN, pD ≈ 1.0): δ = 8.47 (s, 1H; H_4), 8.32 (d, ^3J(H5,H6) = 8.9 Hz, 1H; H_5), 8.20 (br s, 1H; $H_{2'}$), 7.96 (br d, ^3J(H5′,H6′) = 8.7 Hz, 1H; $H_{6'}$), 7.44 (br s, 1H; H_8), 7.34 (br d, ^3J(H5,H6) = 8.9 Hz, 1H; H_6), 7.05 ppm (d, ^3J(H5′,H6′) = 8.7 Hz, 1H; $H_{5'}$); elemental analysis calcd (%) for $C_{15}H_{11}O_9Cl$: C 48.60, H 2.99; found: C 48.55, H 3.04.

Synthesis of F2

This compound was prepared by condensation of 2,4-dihydroxybenzaldehyde (2.0 mmol, 0.276 g) and 3′,4′-dihydroxypropiophenone (2.0 mmol, 0.332 g). The reagents were dissolved in acetic acid (2.5 mL), and 98% H_2SO_4 (0.6 mL) was added. The reaction mixture was stirred overnight. Then, diethyl ether was added and a red solid precipitated. The solid was filtered off and carefully washed with diethyl ether and dried, yielding **F2** (0.517 g, 0.77 mmol, 38%). ^{1}H NMR (DCl/CD_3CN, pD ≈ 1.0) δ = 8.94 (s, 1H; H_4), 8.07 (d, ^3J(H5,H6) = 9.0 Hz, 1H; H_5), 7.75 (d, ^4J(H2′,H6′) = 1.7 Hz, 1H; $H_{2'}$), 7.69 (dd, ^3J(H5′,H6′) = 8.7 Hz, ^4J(H2′,H6′) = 1.7 Hz, 1H; $H_{6'}$), 7.60 (d, ^4J(H6,H8) = 1.8 Hz, 1H; H_8), 7.51 (dd, ^3J(H5,H6) = 8.9 Hz, ^4J(H6,H8) = 1.8 Hz, 1H; H_6), 7.04 (d, ^3J(H5′,H6′) = 8.7 Hz, 1H; $H_{5'}$), 2.72 ppm (s, 3H; 3-CH_3); ^{13}C NMR (DCl/CD_3CN, pD ≈ 1.0): δ = 173.0 (C_2), 170.0 (C_7), 160.2 (C_9), 157.3 (C_4), 154.5 ($C_{4'}$), 147.6 ($C_{3'}$), 133.2 (C_5), 126.7 ($C_{6'}$), 126.1 (C_3), 123.0 (C_6), 122.9 ($C_{1'}$), 120.2 (C_{10}), 118.3 ($C_{2'}$), 117.2 ($C_{5'}$), 102.8 (C_8), 20.3 ppm (CH_3); elemental analysis calcd (%) for $C_{32}H_{30}O_{14}S$: C 57.31, H 4.51, S 4.78; found: C 56.99, H 4.64, S 4.68.

Synthesis of F3

This compound was prepared by condensation of 2,4-dihydroxybenzaldehyde (2.0 mmol, 0.276 g) and 2-chloro-3′,4′-dihydroxyacetophenone (2.0 mmol, 0.373 g). The reagents were dissolved in EtOH (20 mL). The solution was saturated with dry hydrogen chloride for 1 h. The reaction mixture was stirred overnight. Then, the solvent was removed. The red solid that appeared was carefully washed with diethyl ether and dried, yielding **F3** (0.572 g, 1.5 mmol, 77%). ^{1}H NMR (DCl/CD_3CN, pD ≈ 1.0): δ = 9.07 (s, 1H; H_4), 8.03 (d, ^3J(H5,H6) = 8.9 Hz, 1H; H_5), 7.94 (m, 2H; $H_{2'}$, $H_{6'}$), 7.53 (br s, 1H; H_8), 7.50 (dd, ^3J(H5,H6) = 8.9 Hz, ^4J(H6,H8) = 2.2 Hz, 1H; H_6), 7.14 ppm (d, ^3J(H5′,H6′) = 8.5 Hz, 1H; $H_{5'}$); ^{13}C NMR (DCl/CD_3CN, pD ≈ 1.0): δ = 168.7 (C_7), 167.5 (C_2), 158.0 (C_9), 153.7 (C_4), 152.6 ($C_{4'}$), 144.5 ($C_{3'}$), 131.6 (C_5), 126.2 ($C_{6'}$), 122.2 (C_6), 120.9 (C_3), 119.7 ($C_{1'}$), 118.3 (C_{10}), 116.8 ($C_{2'}$), 115.7 ($C_{5'}$), 101.7 ppm (C_8); elemental analysis calcd (%) for $C_{17}H_{16}O_5Cl_2$: C 55.00, H 4.34; found: C 55.34, H 4.01.

Thermodynamic and kinetic studies

The pH jumps were carried out by adding a stock solution of flavylium salt in 1:1 ROH/HCl 0.2 M (1 mL; R = Me or Et) to a 3 mL quartz cuvette containing a solution of 1:1 ROH/NaOH 0.2 M (1 mL), ROH (0.5 mL), and universal buffer of Theorell and Stenhagen (0.5 mL)[31] at the desired final pH. This defined the ionic strength as 0.1 M (controlled by the NaCl concentration resulting from neutralization). The final pH of the solutions was measured in a Crison basic 20 + pH meter. UV/Vis absorption spectra were recorded on Varian Cary 100 Bio or Varian Cary 5000 spectrophotometers. The stopped-flow experiments were conducted in an Applied Photophysics SX20 stopped-flow spectrometer provided with a PDA.1/UV photodiode array detector.

Irradiation experiments

Irradiation experiments were carried out on a spectrofluorimeter Spex Fluorolog 1681 instrument at wavelengths of 370 ($I_0 = 2.8 \times 10^{-7}$ Einstein min^{-1}) or 340 nm ($I_0 = 2.0 \times 10^{-7}$ Einstein min^{-1}). In the case of 3′,4′,7-trihydroxyflavylium, the photochemical experiments were conducted with a Xe–Hg lamp with the irradiation wavelength isolated by using a bandpass filter (Oriel, 366 nm, $I_0 = 1.9 \times 10^{-6}$ Einstein min^{-1}). Light intensity was measured by ferrioxalate actinometry.[32] The flash photolysis experiments were performed on a Varian Cary 5000 spectrophotometer with a Harrick FiberMate attached to the CUV-ALL-UV four-way cuvette holder compartment (Ocean Optics) on the external side of the sample holder to perform light excitation perpendicular to the analyzing beam with the sample compartment shielded with black cardboard and black tape. As a pulsed light source, a commercially available Achiever 630AF camera flash was used, placed in close contact with the sample holder. Excitation was made with the white light of the camera flash with a time resolution of about 0.05 s. Further details were previously described.[33]

Acknowledgements

Financial support from the Fundação para a Ciência e Tecnologia (Portugal) through projects PTDC/QEQ-QFI/1971/2014, UID/QUI/50006/2013 and RECI/BBB-BQB/0230/2012 (co-financed by the ERDF under the PT2020 Partnership Agreement POCI-01-0145-FEDER-007265). A.A.A. thanks the University of Jaén for granting him with a predoc fellowship. N.B. and S.G. acknowledge postdoc grants SFRH/BPD/84805/2012, and SFRH/BPD/111168/2015, respectively.

Keywords: dyes/pigments · kinetics · photochromism · substituent effects · thermodynamics

[1] F. Pina, M. J. Melo, C. A. T. Laia, A. J. Parola, J. C. Lima, *Chem. Soc. Rev.* **2012**, *41*, 869 – 908.
[2] J. G. Sweeny, G. A. Iacobucci, *J. Agric. Food Chem.* **1983**, *31*, 531 – 533.
[3] P. Coggon, G. A. Moss, H. N. Graham, G. W. Sanderson, *J. Agric. Food Chem.* **1973**, *21*, 727 – 733.
[4] R. Brouillard, G. A. Iacobucci, J. G. Sweeny, *J. Am. Chem. Soc.* **1982**, *104*, 7585 – 7590.
[5] R. A. McClelland, S. Gedge, *J. Am. Chem. Soc.* **1980**, *102*, 5838 – 5848.
[6] R. A. McClelland, G. H. McGall, *J. Org. Chem.* **1982**, *47*, 3730 – 3736.
[7] M. J. Melo, A. J. Parola, J. C. Lima, F. Pina, in *Chromic Materials Phenomena and Their Technological Applications* (Ed.: P. R. Somani), Applied Science Innovations Private Limited, **2010**, pp. 537 – 576.
[8] F. Pina, A. J. Parola, R. Gomes, M. Maestri, V. Balzani, in *Molecular Switches, Vol. 1* (Eds.: B. L. Feringa, W. R. Browne), Wiley-VCH, Weinheim, **2011**, pp. 181 – 226.
[9] N. Jordão, R. Gavara, A. J. Parola, *Macromolecules* **2013**, *46*, 9055 – 9063.
[10] S. Gago, I. M. Fonseca, A. J. Parola, *Microporous Mesoporous Mater.* **2013**, *180*, 40 – 47.
[11] Y. Kawano, T. Takenouchi, Y. Kohno, R. Matsushima, M. Shibata, *J. Jap. Soc. Colour Mater.* **2010**, *83*, 289 – 294.

[12] Y. Kohno, M. Ito, M. Kurata, S. Ikoma, M. Shibata, *J. Photochem. Photobiol. A* **2011**, *218*, 87 – 92.
[13] T. Takenouchi, Y. Kawano, Y. Takeuchi, Y. Kohno, K. Takagi, M. Shibata, *J. Jap. Soc. Colour Mater.* **2011**, *84*, 308 – 312.
[14] F. Pina, M. Maestri, V. Balzani, in *Handbook of Photochemistry and Photobiology, Vol. 3* (Ed.: H. S. Nalwa), American Scientific Publishers, **2003**, pp. 411 – 449.
[15] F. Pina, *J. Chem. Soc. Faraday Trans.* **1998**, *94*, 2109 – 2116.
[16] R. Brouillard, B. Delaporte, *J. Am. Chem. Soc.* **1977**, *99*, 8461 – 8468.
[17] R. Brouillard, B. Delaporte, J. E. Dubois, *J. Am. Chem. Soc.* **1978**, *100*, 6202 – 6205.
[18] R. Brouillard, J. Dubois, *J. Am. Chem. Soc.* **1977**, *99*, 1359 – 1364.
[19] F. Pina, in *Recent Advances Polyphenol Research, Vol. 4* (Eds.: A. Romani, V. Lattanzio, S. Quideau), Wiley, Chichester, **2014**, pp. 341 – 370.
[20] F. Pina, *Dyes Pigments* **2014**, *102*, 308 – 314.
[21] F. Pina, *J. Agric. Food Chem.* **2014**, *62*, 6885 – 6897.
[22] G. A. Kraus, Y. Yuan, A. Kempema, *Molecules* **2009**, *14*, 807 – 815.
[23] L. Cabrita, V. Petrov, F. Pina, *RSC Adv.* **2014**, *4*, 18939 – 18944.
[24] M. J. Melo, S. Moura, A. Roque, M. Maestri, F. Pina, *J. Photochem. Photobiol. A* **2000**, *135*, 33 – 39.
[25] F. Pina, M. J. Melo, A. J. Parola, M. Maestri, V. Balzani, *Chem. Eur. J.* **1998**, *4*, 2001 – 2007.
[26] P. Figueiredo, J. C. Lima, H. Santos, M. C. Wigand, R. Brouillard, A. L. Macanita, F. Pina, *J. Am. Chem. Soc.* **1994**, *116*, 1249 – 1254.
[27] N. Basílio, F. Pina, *ChemPhysChem* **2014**, *15*, 2295 – 2302.
[28] A. L. Maçanita, F. Pina, J. C. Lima, *Biotecnol* **1997**, *56*, 4 – 13.
[29] A. Roque, C. Lodeiro, F. Pina, M. Maestri, R. Ballardini, V. Balzani, *Eur. J. Org. Chem.* **2002**, 2669 – 2709.
[30] A. Robertson, R. Robinson, *J. Chem. Soc.* **1928**, 1460 – 1472.
[31] F. W. Küster, A. Thiel, E. Brückner, *Tabelle per Le Analisi Chimiche e Chimico-fisiche*, Hoepli, Milano, **1985**, 157 – 160; the universal buffer used was prepared in the following way: 85 % (w/w) phosphoric acid (2.3 cm^3), monohydrated citric acid (7.00 g), and boric acid (3.54 g) were dissolved in water; 1 M NaOH (343 mL) was then added, and the solution was diluted to 1 dm^3 with water.
[32] C. G. Hatchard, C. A. Parker, *Proc. R. Soc. A Math. Phys. Eng. Sci.* **1956**, *235*, 518 – 536.
[33] M. Maestri, R. Ballardini, F. J. S. Pina, M. J. Melo, *J. Chem. Educ.* **1997**, *74*, 1314 – 1316.

Received: April 4, 2016
Published online on July 28, 2016